Original Paper

SCIENTIAFUNGORUM

DOI: 10.33885/sf.2024.55.1457
(2024) Vol. 55: e1457

Talaromyces oaxaquensis sp. nov. section *Talaromyces* (Trichocomaceae, Eurotiales) isolated from pseudostems of banana plants in Mexico

Talaromyces oaxaquensis sp. nov. sección *Talaromyces* (Trichocomaceae, Eurotiales) aislada de pseudotallos de plantas de plátano en México

Aneliz de Ita Zárate-Ortiz[1], José Luis Villarruel-Ordaz[1], Ana Claudia Sánchez-Espinosa[1], Luis David Maldonado-Bonilla[2]

[1] Institute of Genetics, Universidad del Mar Campus Puerto Escondido, Puerto Escondido, C.P. 71980, Oaxaca, Mexico.
[2] CONAHCYT Research Fellow, Institute of Genetics, Universidad del Mar Campus Puerto Escondido, Puerto Escondido, C.P. 71980, Oaxaca, Mexico.

RESUMEN

Antecedentes: *Talaromyces* es un género de Eurotiales que se divide en ocho secciones. Las especies se adaptan a diferentes hábitats como el suelo, alimentos procesados, pacientes inmunocomprometidos y plantas.

Objetivo: Identificar tres aislados de *Talaromyces* provenientes de pseudotallos de *Musa* sp. AAB 'Manzano'.

Métodos: Se analizó la morfología de las colonias de *Talaromyces* en medios recomendados, las ascosporas se observaron bajo microscopía electrónica de barrido y se realizó una filogenia del concatenado ITS-*RPB1*-*RPB2*.

Resultados y conclusiones: Las tres cepas se agrupan en un mismo clado dentro de la sección *Talaromyces*, siendo *T. rubicundus* la especie más cercana. La morfología, color y crecimiento de los aislados es distinguible de *T. rubicundus* y otras especies relacionadas. No se detectó la formación de conidios bajo ninguna condición, pero se producen cleistotecios en un medio de agar y avena, los cuales albergan ascas con ascosporas ornamentadas con espinas. Se propone que estas cepas son representativas de *Talaromyces oaxaquensis* sp. nov.

Palabras clave: Ascomicetos, Eurotiales, endófito, Oaxaca

ABSTRACT

Background: *Talaromyces* is a genus of Eurotiales divided into eight sections. The species are adapted to habitats such as soil, processed foods, immunocompromised patients, and plants.

Objective: Identify three *Talaromyces* isolating from pseudostems of *Musa* sp. AAB 'Manzano'.

Methods: The morphology of *Talaromyces* colonies in recommended media was analyzed, ascospores were observed under scanning electron microscopy, and a phylogeny of the concatenated ITS-*RPB1*-*RPB2* was performed.

Results and conclusions: The three strains are clustered in the same clade within the section *Talaromyces*, being *T. rubicundus* the most related species. The isolates morphology, color, and growth rate are distinguishable from *T. rubicundus* and other related species. No conidia formation was detected under any conditions, but cleistothecia are widely produced on an oatmeal-agar medium, which harbors asci with ascospores with spiny ornamentation. We propose these strains are representative of *Talaromyces oaxaquensis* sp. nov.

Keywords: Ascomycetes, Eurotiales, endophyte, Oaxaca

ARTICLE HISTORY

Received: 12 February 2024
Accepted: 27 August 2024
On line: 9 September 2024

CORRESPONDING AUTHOR

Luis David Maldonado Bonilla, email: maldonado@zicatela.umar.mx
Orcid: 0000-0001-6515-1983

INTRODUCTION

The *Talaromyces* genus (Eurotiales) comprises species displaying anamorphic or teleomorphic states. Anamorphs were initially classified into *Penicillium* subgenus *Biverticillium*, and *Talaromyces* only included species with teleomorph state (Pitt 1979). Although the anamorphic state and production of green conidia observed in *Talaromyces* might be visually reminiscent of *Penicillium*, both are independent genera of Eurotiales families (*Trichocomaceae* and *Asgergillaceae*, respectively) (Yilmaz *et al*. 2014). The sexual state of *Talaromyces* is distinguished by a yellow ascomata covered with interwoven hyphae that produce globose asci containing subglobose to ellipsoidal ascospores, mainly ornamented (Houbraken *et al*. 2020).

The first classification of *Talaromyces* sensu stricto was composed of 88 accepted species divided into seven sections, the section *Talaromyces* being the most diverse (Yilmaz *et al*. 2014). Since then, 12 new species isolated in China have been reported (Sun *et al*. 2020, Wei *et al*. 2021, Sun *et al*. 2022, Wang *et al*. 2022), and one of those species (*T. tenuis*) belongs to a new section (Sun *et al*. 2020). The species of *Talaromyces* are versatile as they have been isolated from different habitats and organisms, such as soil, freshwater, decayed wood, processed food and beverages, stored grains, insect galls, immunocompromised patients, and plants (Yilmaz *et al*. 2014).

Several *Talaromyces* spp. have been isolated from living and decaying plants, but in any case, they are reported as phytopathogens (Yilmaz *et al*. 2014). *Talaromyces pinophilus* CBS 440.89 and *T. radicus* CBS 100490 have been isolated from maize and wheat respectively (Yilmaz *et al*. 2014). *Talaromyces pinophilus* F36CF is also an endophytic strain isolated from the strawberry tree (*Arbutus unedo*) (Vinale *et al*. 2017). Fungal endophytes can promote plant growth, increase tolerance to stresses, and antagonize the growth of phytopathogens (Lugtenberg *et al*. 2016). However, the beneficial features of *Talaromyces* endophytes are unknown.

Bananas and plantains are the fruits of different cultivars of the perennial plant *Musa* sp. Cultivation is an essential economic activity in developing countries with tropical climates. Banana production and exports have declined from 20.4 million tons in 2021 to 19.1 million tons in 2022 due to adverse weather conditions, insufficient access to fertilizers, and the outbreak of the fungal pathogen *Fusarium oxysporum* f. sp. *cubense* tropical race 4 (FAO 2022). This downward trend might continue in the following years. Plant-associated microbes might improve plant growth and health, mainly native microbes adapted to the conditions where the plants grow. In this context, the novel species *Talaromyces oaxaquensis* was identified while searching for fungal endophytes of banana plants. This is the first report of an endophyte Talaromyces associated with banana plants that contributes to the knowledge of this genus, which has yet to be studied in Mexico. It will also set research focused on *Talaromyces*-plant interaction.

MATERIALS AND METHODS

Fungal isolation

Plants of *Musa* sp. AAB 'Manzano' coming from a micropropagation protocol (Maldonado-Bonilla *et al*. 2019) were transferred at the 6-leaves stage into the soil of the grounds belonging to the Universidad del Mar at Puerto Escondido, Mexico. After 8 months, pieces of pseudostems of approximately 15 cm in length were removed and stored in FalconTM 50 mL tubes. Once in the pseudostems were washed with running water and dissected into square pieces of 2 cm^2. These fragments were surface sterilized by soaking them in 70 % ethanol for 1 min, followed by a 10 min treatment with a commercial bleaching solution with an actual concentration of 0.54 % sodium hypochlorite and 3 washes of 10 min with sterile water. Once disinfected, the fragments of pseudostems were placed in Potato-Dextrose Agar (PDA) plates supplemented with 200 mg mL^{-1} of ampicillin to prevent bacterial growth. The plates were incubated at 25 °C for 7 days in the dark. The mycelia that were able to grow in this condition were placed separately in fresh PDA plates. Three specimens denoted N10, N11, and N12, showed similar morphological features; everyone came from an independent plant. These fungi produced ascospores over three weeks of incubation in PDA at 25 °C in darkness. Serial dilutions of ascospores harvested in water were plated into PDA plates and incubated for 3 days at 25 °C in darkness. Emerging hyphae of each strain were picked and sown into fresh PDA plates to obtain monosporic cultures.

Morphological analysis

The strains N10, N11, and N12 were grown in Czapek Yeast Extract Agar (CYA) and Malt Extract Agar (MEA). Three PDA blocks were inoculated in plates of each tested media and incubated in darkness at 25 °C. A set of CYA plates was also incubated in darkness at 37 °C. Three independent biological replicates were performed to estimate the growth rate and describe its morphology after one week of incubation (Yilmaz *et al*. 2014). Oatmeal Agar (OA) was also tested as it stimulates the transition to the sexual state (Yilmaz *et al*. 2014, Wei *et al*. 2021). OA was prepared by boiling 15 g of rolled oat in 500 mL of water. The liquid was filtered, mixed with 10 g of Bacto agar, and autoclaved. Microscopical descriptions of ascoma and ascospores were made from samples of two-week-old cultures grown in OA in darkness at 25 °C stained with lactophenol-cotton blue and observed by optical microscopy in a Primo Star microscope (Carl Zeiss, Oberkochen, Germany) equipped with a Canon PowerShot G16 digital camera. The size of asci and ascospores was determined using TuopView 3.7 software (ToupTek Photonics Co., Ltd). Ascospore ornamentation was observed under a scanning electron microscope (Hitachi SU 1510, Dallas, United States of America).

Genomic DNA extraction and amplification

Genomic DNA from frozen and grounded mycelium of N10, N11, and N12 were extracted with an EZ-10 Spin Column Genomic kit. DNA was diluted to 10 ng μL^{-1} to perform the amplification of a fragment encompassing the 3' end of the Small Subunit Ribosomal RNA, the complete Internal Transcribed Spacer region (ITS) (ITS1-5.8S ribosomal RNA-ITS2), and a fragment of the Large Subunit Ribosomal RNA (LSU) by using the oligonucleotide combination ITS1F (5'-CTTGGTCATTTAGAGGAAGTAA-3') and LR5 (5'-TCCTGAGGGAAACTTCG-3'). MyTaq polymerase (Meridian Bioscience, Cincinnati, United States of America) was used to perform the PCR with the following conditions: 95 °C for 4 min as initial denaturation, 35 cycles of 94 °C for 60 s, 54 °C for 30 s and 72 °C for 90 s, and 72 °C for 5 min as a final extension step. PCR products were separated and visualized by electrophoresis in 1 % agarose gels with GelGreenR stain. Amplicons were cloned into plasmids and sequenced with universal M13 primers by the capillary electrophoresis sequencing service of Macrogen (Seoul, Korea). Sequences were assembled from the electropherograms visualized in Chromas 2.6.2 (Technelysium). The sequences were submitted to GeneBank and are available under the accession numbers OR449219, OR449220, and OR449221. Phylogenetically informative fragments of *RPB1* and *RPB2* were amplified with the oligonucleotide combination TalaRPB1F (5'-TTGTNTCGCCACAGAGAAAYG-3') and TalaRPB1R (5'-AACCTTCGTTTCWAAYGTCT-3') for *RPB1*, and fRPB2-5F (5'-GAYGAYMGWGATCAYTTYGG-3') combined with bRPB2-7R (5'-GAYTGRRTRTGRTCRRGGAAVGG-3') to amplify *RPB2*. For both fragments, the PCR conditions were 93 °C for 2 min, 35 cycles of 93 °C for 1 min, 50 °C for 1 min, 72 °C for 1 min, with a ramp rate of 2 s/cycle and a final extension of 72 °C for 10 min (Matheny 2005). The sequencing strategy of these amplicons was the same as described above. The GeneBank accession numbers of the *RPB1* and *RPB2* sequences are available at GeneBank under the accession numbers OR605592 to OR605597.

Phylogenetic analysis

The MAFFT program v.7 (Katoh *et al*. 2019) was used to align the DNA sequences of the ITS region, *RPB1*, and *RPB2* of the isolates N10, N11, and N12 together with the corresponding sequences of *Talaromyces* type strains from the sections *Talaromyces*, *Purpuei*, and *Helici*, and well as *Trichocoma paradoxa* as outgroup (Yilmaz *et al*. 2014). The accession numbers of the sequences used in the phylogenetic analysis are included in Table 1. The trimmed alignments were concatenated and subject to Bayesian inference in MrBayes 3.2.7 by selecting the General Time Reversible model with two sets of four chains (one cold, three heated) until an average deviation of frequency reached 0.01 (Ronquist *et al*. 2012). The sampling frequency was 100, and the first 25 % of trees were removed as burn-in. The phylogenetic tree was edited in MEGA X (Kumar *et al*. 2018). The ITS region of N10, N11, and N12, together with sequences of type and reported strains, were aligned by ClustalW to later reconstruct a maximum-likelihood phylogeny with 1000 Bootstrap replicates with PhyML 3.0 (Guindon *et al*. 2010). The best substitution model was selected with the Smart Model Selection of PhyML (Lefort *et al*. 2017) and the tree was edited in MEGA X (Kumar *et al*. 2018).

Table 1. Accession numbers of the sequences obtained in this study and sequences from type strains used in the phylogenetic analysis. Names are presented in alphabetic order

Name	ITS	*RPB1*	*RPB2*
N10	OR449219	OR449220	OR44922119
N11	OR605592	OR605593	OR605594
N12	OR605595	OR605596	OR605597
Talaromyces amestolkiae DTO179F55	JX315660	JX315679	JX315698
Talaromyces apiculatus CBS 312.59	JN899375	JN680293	KM023287
Talaromyces boninensis CBS 650.95	JN899356	JN680319	KM023276
Talaromyces derxii CBS 412.89	JN899327	JN680306	KM023282
Talaromyces duclauxii CBS 322.48	JN899342	JN121643	JN121491
Talaromyces funiculosus CBS 272.86	JN899377	JN680288	KM023293
Talaromyces helicus CBS 335.48	JN899359	JN680300	KM023273
Talaromyces macrosporus CBS 317.63	JN899333	JN680296	KM023292
Talaromyces primulinus CBS 321.48	JN899317	JN680298	KM023294
Talaromyces purpureus CBS 475.71	JN899328	JN121687	JN121522
Talaromyces purpurogenus CBS 286.36	JN899372	JN680271	JX315709
Talaromyces rubicundus CBS 342.59	JN899384	JN680301	KM023296
Talaromyces stipitatus CBS 375.48	JN899348	JN680303	KM022380
Talaromyces viridis CBS 114.72	AF285782	JN121571	JN121430
Talaromyces viridulus CBS 252.87	JN899314	JN680284	JF417422
Trichocoma paradoxa CBS 103.73	MH872339	JN121558	JN121417

RESULTS

Morphological identification

Identifying sulcate and white mycelium with a yellowish-brown color at the reverse in PDA plates was the early criteria to set that the fungi N10, N11, and N12 isolated from independent banana plants share the same morphotype. When inoculated in CYA at 25 °C, the colonies of the isolates are white, floccose to velvety, and slightly sulcate. The reverse is brown but fades to yellow at the border. The sulcation and the color fading are not evident when growing at 37 °C. Colonies in MEA are floccose to velvety, the reverse color is also brown and fades into pastel yellow at the border (Figure 1). No pigments diffuse throughout the agar. Description of colonies and measurements of growth rate are shown in Table 2. Species of *Talaromyces* section *Talaromyces* produce conidiophores and even synnemata in the tested media, a critical parameter to species identification. However, none of the isolates produced such structures even after prolonged incubation, although closed ascomata of the cleistothecium type were usually observed after three weeks of incubation (data not shown).

Massive production of yellow cleistothecia was observed after two weeks of incubation in OA (Figure 2),

even the vegetative mycelia is hardly detectable on this condition. The cleistothecia released asci endowed with a thin envelope containing 5 to 7 ascospores (Figure 2). Asci and subglobose to ellipsoidal one-celled ascospores released from the ascomata were observed by optical microscopy (Figure 2). The ascospores tend to be aggregated; thus, resuspension in water helps separate them. As the thick wall of the ascospores did not allow the resolution of their surface, the ascospores were subject to SEM. Ascospores are fully covered by spines of over 0.5 µm long (Figure 2). Description of the structures of sexual state and dimensions are presented in Table 3. The sexual state is limited to certain species; thus, *T. flavus, T. macrosporus,* and *T. paucisporus* were included as references in Table 3 (Yilmaz *et al*. 2014). The anamorphs of *T. flavus* and *T. macrosporus* are known, while *T. paucisporus*, like N10, N11, and N12, lack sexual states, but asci and ascospores dimensions are quite different (Table 3).

Once the sequences of the ITS region and the LSU were obtained, they were submitted separately as queries to search for similar sequences in the GeneBank of the National Center for Biotechnology Information (NCBI) by using the BLASTN algorithm to confirm that N10, N11, and N12 belong to the *Talaromyces* genus (data not shown). Afterwards, the phylogenetically informative fragments of *RPB1* and *RPB2* were obtained for the subsequent phylogenetic analysis of the concatenate ITS-*RPB1*-*RPB2* of the isolates N10, N11, and N12 together with the corresponding sequence of type strains and *Trichocoma paradoxa* as outgroup (Yilmaz *et al*. 2014). The phylogeny presented in Figure 3 shows that these novel isolates form an independent clade within the section *Talaromyces* with high bootstrap values and posterior probabilities, and *T. rubicundus, T. pinophilus, T. amestolkiae,* and *T. apiculatus,* the most related species, but distinguishable from N10, N11, and N12.

A further maximum-likelihood phylogeny of the ITS barcode region that included type and reported sequences, the sequences of the recently reported species of the section *Talaromyces: T. brevis, T. sparsus, T. aurelolinus,* and *T. nanjingensis* (Sun *et al*. 2020, Wei *et al*. 2021, Sun *et al*. 2022) as well as strains the above-mentioned *T. flavus, T. macrosporus,* and *T. paucisporus* whose sexual state. Sequences of the isolates HR8-5 and HR8-8 were included as they are reported as related to *T. rubicundus* (Maneeboon *et al*. 2023). The isolates were again clustered in this maximum-likelihood phylogeny, and *T. rubicundus* was the most related sequence (Figure 4).

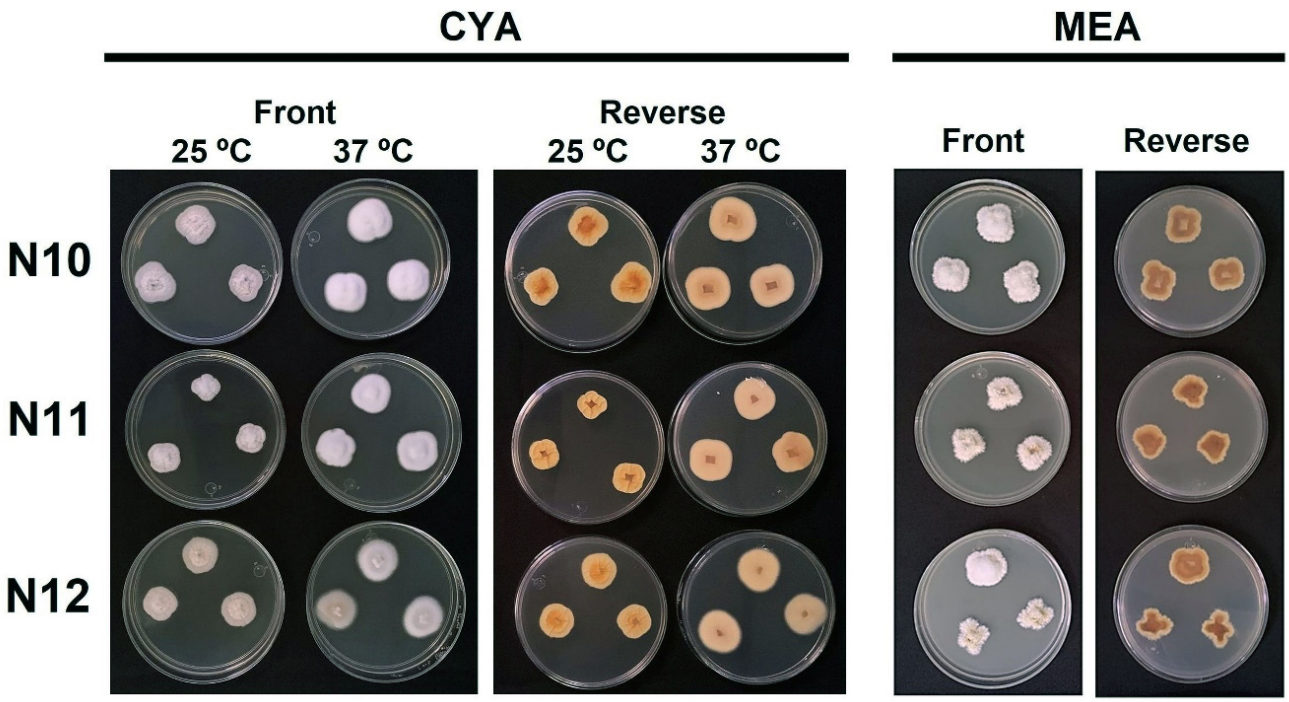

Figure 1. Morphological features of the strains N10, N11, and N12. Aspect of the colonies growing in CYA and MEA.

Table 2. Growth rates and morphological features of colonies of the isolates N10, N11, and N1 compared to phylogenetically related species

Name	Growth rate in CYA (mm)			Anamorph description	CYA colony texture (25 °C)	CYA reverse color (25 °C)	MEA colony texture (25 °C)	MEA reverse color (25 °C)
	CYA, 25 °C	CYA, 37 °C	MEA, 25°C					
N10	16-24	21-28	None	None	Raised at centre, floccose to velvety, slightly sulcate	Brown in the centre, fades o yellow at the border	Raised at centre, floccose to velvety	Brown, fading into pastel yellow
N11	15-22	22-24	None	None				
N12	17-24	24-34	None	None				
T. apiculatus	38-41	25-35	40-42	Biverticilate conidiophore and globose conidia	Moderately deep, radially and concentrically sulcate	Greyish yellow to yellowish white	Floccose to strongly funicu-lose	Brownish orange
T. amestolkiae	30 -32	8 - 15	30 - 45	Biverticilate conidiophore and ellipsoidal conidia	Floccose to overlaying funi-culose	Violet brown	Plane, slightly raised at centre	Dark brown
T. pinophilus	18 - 25	25 -40	30 -40	Biverticilate conidiophore and globose to subglobose conidia	Raised at centre, sulcate	Greyish orange to orange	Loosely funiculo-se to floccose	Brownish orange
T. rubicundus	30 -32	24 - 34	38 -39	Biverticilate conidiophore and subglobose to ellipsoidal conidia	Raised at centre, sulcate	Brownish orange in the centre, fades to whitish orange	Floccose	Brown, fading into brownish orange

Data from related species were taken from Yilmaz *et al*. (2014).

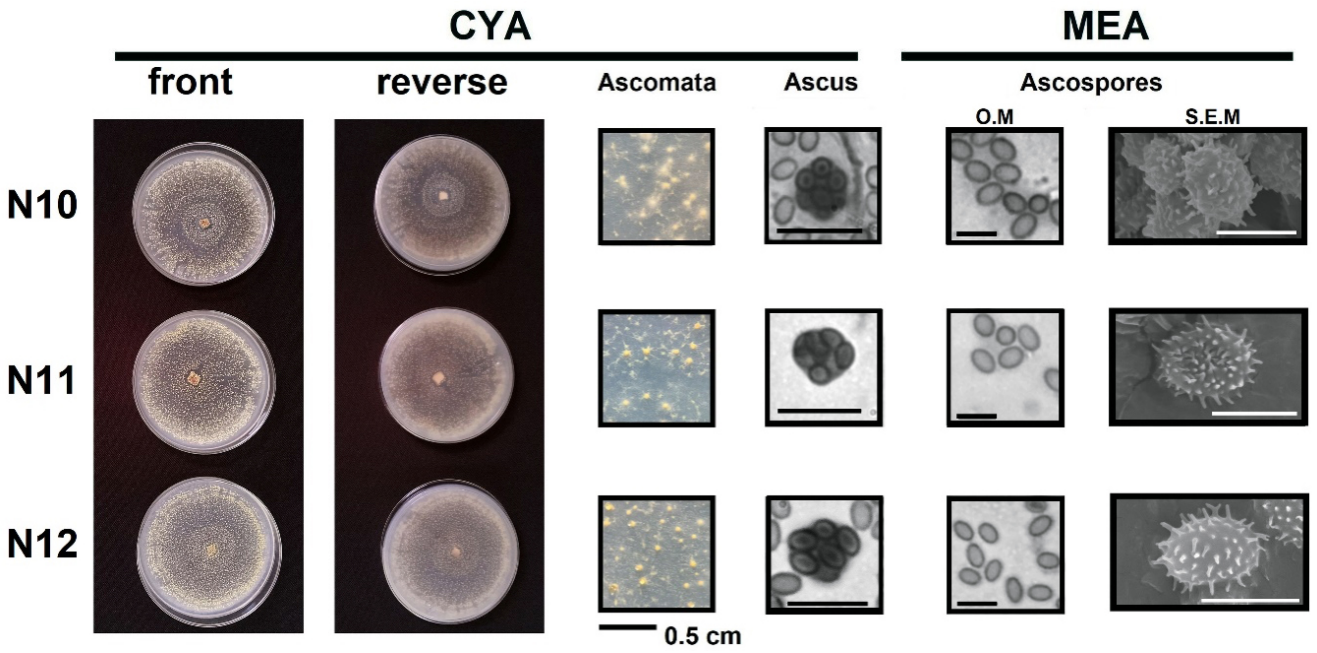

Figure 2. Macroscopical and microscopical characters of the strains growing in oatmeal agar where asci and ascospores are produced.Yellow cleistothecia (ascomata) are visualized under this condition. Asci and ascospores were visualized by optical microscopy (OA), cotton blue staining, scale bars 10 µm and 5 µm, respectively. Spiny ascospores were also visualized by scanning electron microscopy (SEM), scale bars 3 µm.

Table 3. Dimensions of asci and ascospores and characteristics of ascospores of N10, N11, N12 and reference species

Isolate	Asci length × height (µm)	Ascospore length × height (µm)	Ascospore shape	Ornamentation
N10	6.4-9.5 × 6.6-7.9	2.5-4.4 × 2.1-2.8	Subglobose to ellipsoidal	Spiny
N11	6.8-8.1 × 6.1-7.5	2.7-4.9 × 2.2-3.2	Subglobose to ellipsoidal	Spiny
N12	7.8-8.2 × 5.7-7.5	2.3-4.9 × 2.0-3.2	Subglobose to ellipsoidal	Spiny
T. flavus	9.5-13.5 × 8.0-11.5	4.0-5.5 × 3.0-3.4	Broadly ellipsoidal	Spiny
T. macrosporus	13.0-15.0 × 11.5 x 13.5	5.0-6.5 × 4.5-5.5	Subglobose to broadly ellipsoidal	Spiny
T. paucisporus	22.0-25.0 × 18.0-22.0	14.0-18.0 × 12.0-16.0	Subglobose to broadly ellipsoidal	Spiny

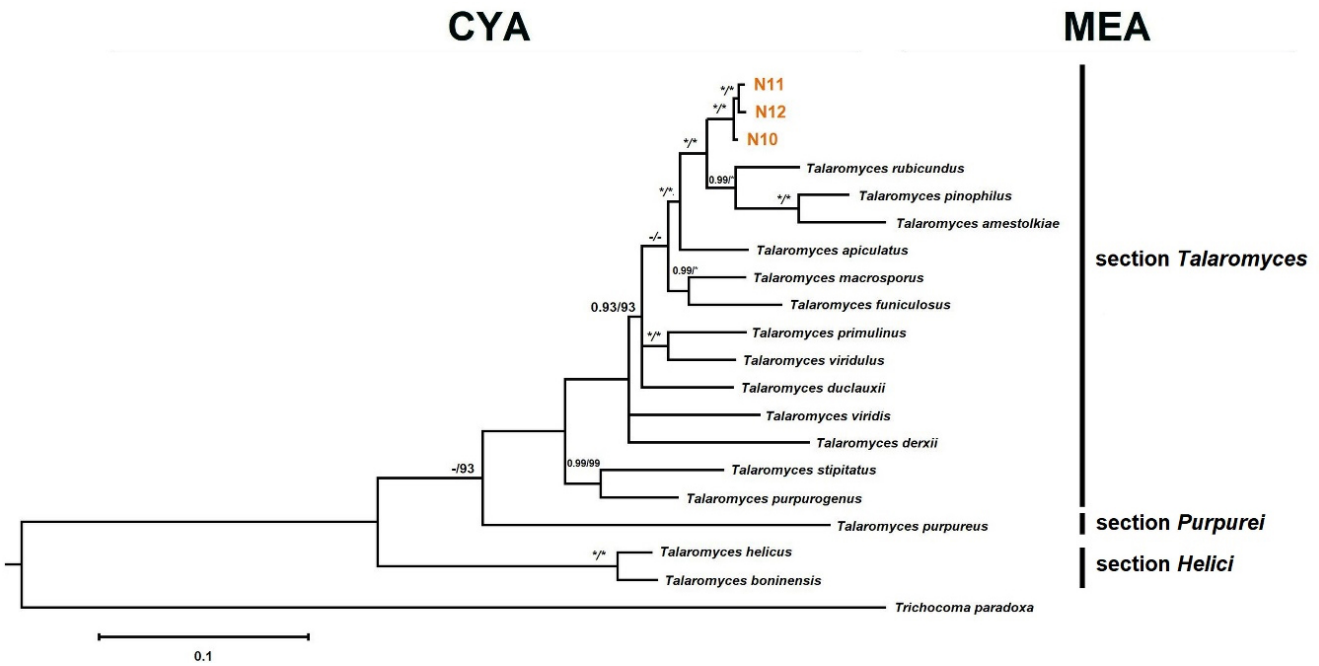

Figure 3. Phylogeny of the concatenated markers ITS, *RPB1*, and *RPB2* from the isolates N10, N11, and N12 and representative type strains of the *Talaromyces, Purpurei*, and *Helici sections*. *Trichocoma paradoxa* was used as outgroup. Above the internodes, posterior probabilities (Bayesian inference analysis) and bootstrap values higher than 0.7 and 70 %, respectively, are indicated. Support values (1/100 %) are indicated by asterisks (*).

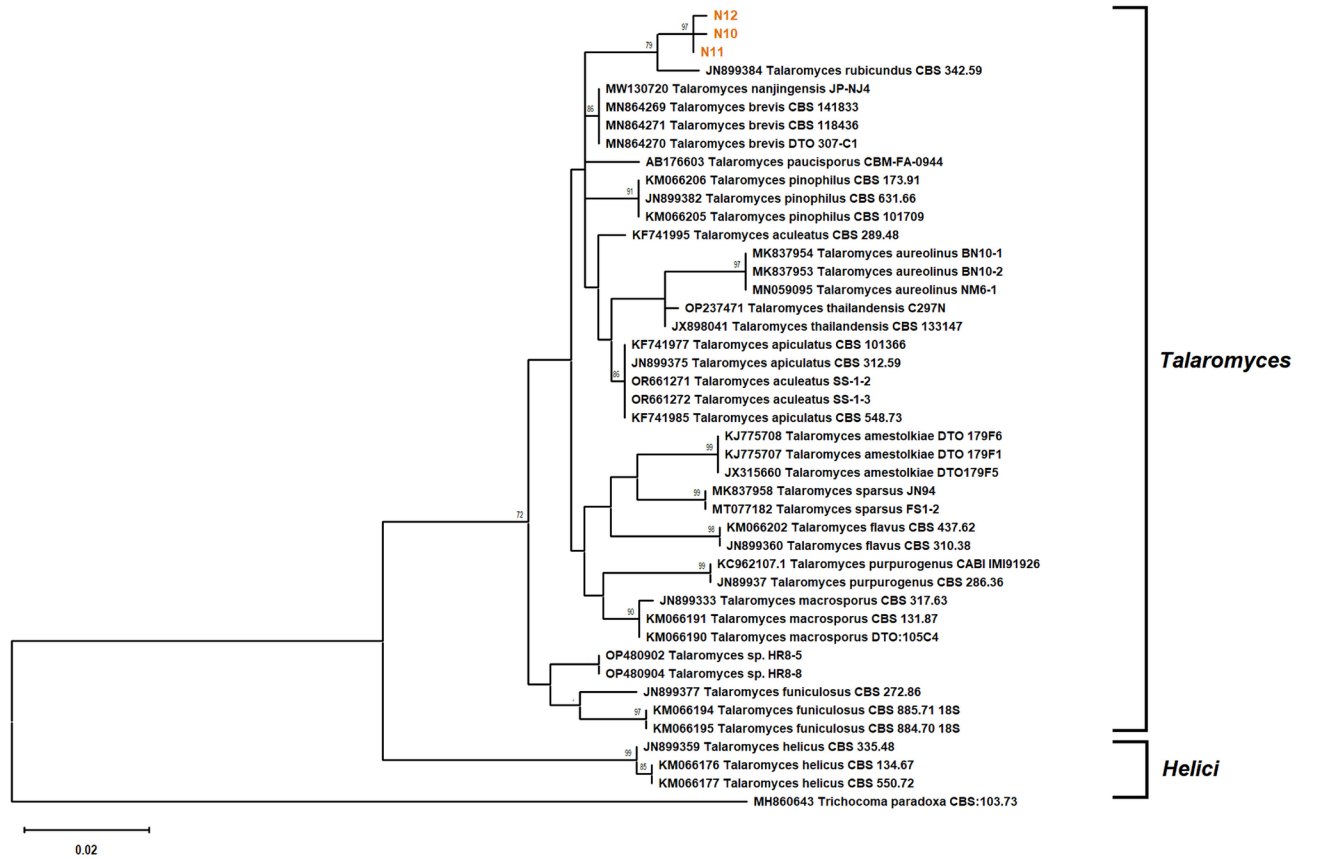

Figure 4. Maximum-likelihood phylogeny of sequences of the ITS region of N10, N11, N12, type strains, and selected isolates, including recently reported species of section *Talaromyces* (see text for details). The TN93 + I was chosen as the best substitution model, and the bootstrap values of numbers above 70 are indicated above the branches. The accession numbers of each sequence are shown on the left side of the species name. Sequences from type strains are marked by the "T" as superindex at the right of the accession number.

DISCUSSION

The wide range of niches where *Talaromyces* is established reveals the endowed adaptations of those fungi to colonize such habitats and interact with other organisms, which might influence the emergence of new species in the long term. Plants are niches colonized by *Talaromyces* spp.; thus, such species are endowed with factors that enable plant growth and their surrounding environment. Potential benefits in the plants might positively impact the natural selection of *Talaromyces* spp. The endophytic growth of *Talaromyces* is possible as some strains from the section *Talaromyces*, such as *T. pinophilus* CBS 440.89 and *T. radicus* CBS 100490, have been isolated from maize and wheat plants, respectively (Yilmaz *et al*. 2014). *Talaromyces pinophilus* F36CF is also an endophytic strain isolated from the strawberry tree (*Arbutus unedo*) (Vinale *et al*. 2017). *Talaromyces flavus* is a resident of soil from potato fields (Naraghi *et al.* 2012), and *T. nanjingensis* is associated with the rhizosphere of *Pinus massoniana* (Sun *et al*. 2022). The physical closeness of *T. flavus* and *T. nanjingensis* to plants is another evidence of the adaptation to niches where cultivated plants have influence. Due to the high diversity of microbes in the soil, the potential of the strains of *Talaromyces* N10, N11, and N12 to interact with plants via roots and eventually have endophytic growth might secure space to growth and uptake photosynthates and micronutrients from the plant. Although it is unknown how they accessed the plants, each isolate comes from an independent plant, which suggest that they colonize vegetation as a strategy of adaptation.

The morphology of the colonies growing into CYA and MEA illustrated that they have the expected species features from the section *Talaromyes*. Still, the three isolates grew slower in MEA than the related species (Figure 1, Table 2). The sulcation is a shared feature, but the colonies of N10, N11, and N12 have a floccose to velvety aspect, and the reverse color in CYA and MEA are distinguishable from the other species (Table 2). The anamorph is a common feature in the species of the section *Talaromyces*. The conidia of *Talaromyces* spp. are primarily green, reminiscent of *Penicillium* spp., and produced whether in CYA or MEA (Houbraken *et al*. 2020). However, conidiation of *T. flavus* is seldom detectable (Yilmaz *et al*. 2014). Like N10, N11, and N12, the conidiation of *T. intermedius* (section *Talaromyces*) is absent in CYA and MEA, but it was stimulated in the Hay Infusion Agar (Yilmaz *et al*. 2014). We could not test Hay Infusion Agar in N10, N11, and N12, and no candidate molecules that might trigger conidiation as the composition of CYA and MEA is complex. We also tested minimal M9 medium, liquid potato-sucrose medium, and mechanical damage to stimulate conidiation, but it was not stimulated (data not shown). *Talaromyces mimosinus* (section *Bacilliospori*) produces conidiophores when growing in OA, a paradoxically stimulant of ascospore production (Yilmaz *et al*. 2014). These examples suggest that particular species of *Talaromyces* have peculiar requirements to induce conidiation, which is the case of N10, N11, and N12. Identification of conidiation-related genes in N10, N11, and N12 and their comparison between *T. intermedius, T. flavus,* and species competent to conidiate might help to explain the differences in the ability to conidiate among *Talaromyces* spp.

OA induced the formation of ascoma of N10, N11, and N12 (Figure 2). Spiny ornaments of the subglobose to ellipsoidal ascospores were visualized by SEM (Figure 2). The shape of ascospores varies among species of *Talaromyces*, but the spines are the most recurrent ornaments up to 0.4 µm long. The shape and ornaments of N10, N11, and N12 ascospores coincide with those reported in *T. macrosporus, T. flavus,* and *T. derxii*. However, such species are not closely related and produce conidiophores and conidia.

The phylogenetic analysis illustrates that the strains N10, N11, and N12 are clustered together and belong to the section *Talaromyces* (Figure 3). The strains form a clade independent of *T. rubicundus, T. pinphilus, T. amestolkiae*, and *T. apiculatus*, the most related ones (Figure 3). The maximum-likelihood phylogeny of the ITS region confirmed the close relationship between isolated N10, N11, and N12 (Figure 4). This phylogeny included sequences related to N10, N11, and N12 form-type strains and isolates whose *RPB1* and *RPB2* sequences are unknown. Like in the concatenated tree, *T. rubicundus* was the most related sequence. The ITS sequence of *T. paucisporus* was included in this phylogenetic analysis as it lacks an asexual state but shows yellow cleistothecia and spiny ascospores (Yilmaz *et al*. 2014).

The ITS sequences of the isolates HR8-5 and HR8-8 from pineapple fields were included in this phylogenetic analysis since, likewise, the sequences of the isolates N10, N11, and N12 are related to *T. rubicundus* (Maneeboon *et al.* 2023). We did not find further reports of ITS sequences of *T. rubicundus*. In the maximum-likelihood phylogeny presented here, HR8-5 and HR8-8 are not clustered with *T. rubicundus*, N10, N11, or N12; they are instead grouped with sequences of *T. funiculosus* (Figure 4). The selection of the phylogenetic reconstruction method caused discrepancies in these results, as the neighbor-joining method was initially used to reconstruct the phylogenetic tree of HR8-5 and HR8-8 (Maneeboon *et al.* 2023). However, the phylogenetic reconstruction of the ITS sequences confirmed that N10, N11, and N12 form an independent clade related to the type strain of *T. rubicundus.*

The sexual state is lacking in the phylogenetically related species *T. rubicundus, T. pinophilus, T. amestolkiae,* and *T. apiculatus* (Yilmaz *et al.* 2014). Hence, the characteristic production of cleistothecia by N10, N11, and N12 is a feature that allows the clear distinction of these isolates concerning the phylogenetically related species. The three strains presented here are proposed to be homothallic as the ascoma emerged by the sole inoculation of one isolate, which is consistent with most of the *Talaromyces* species with described sexual stage. Species of the section *Talaromyces*, such as *T. marneffei* and *T. pinophilus*, have the MAT-1 and MAT-2 loci, but the heterothallism has yet to be reproduced under laboratory conditions (Henk *et al.* 2012). Further identification of MAT loci in the strains presented here and in the related species is necessary to clarify the mechanisms of reproduction of these fungi.

Species of *Talaromyces* have been identified in Mexico. *Talaromyces rotundus* (section *Islandici*) and *T. ocotl* (*Sagenomella ocotl*) were isolated from the soil of the Volcanic Cordillera of Veracruz (Heredia *et al.* 2001). *T. ocotl* is currently excluded from the list of *Talaromyces* spp. as *Sagenomella* is an independent genus of *Trichocomaceae*. *Talaromyces verruculosus* (section *Talaromyces*) was isolated from stored seeds of groundnut, which caused storage rot; only the anamorph was observed (Ortega-Acosta *et al.* 2018). Although possible, these two reports do not consider the association of such species with physiologically active plant tissue. The new species isolated in Mexico and presented here could acquire factors in the curse of evolution to enable the colonization of banana plants, an essential crop in countries with tropical climates. Colonization of plant tissues contributes to avoiding competition with other microbes in the soil and facilitates the uptake of carbon sources from the plant. The elucidation of the effects on the plants will be a future task.

CONCLUSION

The current knowledge of the *Talaromyces* genus might be a glimpse of a more diverse genus. To our knowledge, we presented here, for the first time, three endophytic specimens of *Talaromyces* isolated from banana plants growing in Oaxaca, Mexico. The phylogenetic and morphological analyses revealed that they belong to a novel species from the section *Talaromyces*, lacking the anamorph state but forming ascomata in oatmeal agar, which releases spiny ascospores. We propose *Talaromyces oaxaquensis* represents a new species whose name refers to the Mexican state where those specimens were isolated.

REFERENCES

FAO. 2022. Banana market review 2022. Food Agricultural Organization of the United Nations. https://www.fao.org/3/cc6952en/cc6952en.pdf (May 1, 2023).

Guindon S, Dufayard JF, Lefort V, Anisimova M, Hordijk W, Gascuel O. 2010. New algorithms and methods to estimate maximum-likelihood phylogenies: assessing the performance of PhyML 3.0. Systematic Biology 29, 307-321. https://doi.org/10.1093/sysbio/syq010

Henk DA, Shahar-Golan R, Devi KR, Boyce KJ, Zhan N, Fedorova ND, Nierman WC, Hsueh PR, Yuen KY, Sieu TP, Kinh NV. 2012. Clonality despite sex: the evolution of host-associated sexual neighborhoods in the pathogenic fungus *Penicillium marneffei*. PLoS Pathogens 8, e1002851. https://doi.org/10.1371/journal.ppat.1002851

Heredia G, Reyes M, Arias RM, Bills GF. 2001. *Talaromyces ocotl* sp. nov. and observations on *T. rotundus* from conifer forest soils of Veracruz State, Mexico. Mycologia 93, 528-540. https://doi.org/10.1080/00275514.2001.12063185

Houbraken J, Kocsubé S, Visagie CM, Yilmaz N, Wang XC, Meijer M, Kraak, B, Hubka V, Bensch K, Samson RA, Frisvad JC. 2020. Classification of *Aspergillus, Penicillium, Talaromyces* and related genera (Eurotiales): An overview of families, genera, subgenera, sections, series and species. Studies in Mycology 95, 5-169. https://doi.org/10.1016/j.simyco.2020.05.002

Katoh K, Rozewicki J, Yamada KD. 2019. MAFFT online service: multiple sequence alignment, interactive sequence choice, and visualization. Briefings in Bioinformatics 20, 1160-1166. https://doi.org/10.1093/bib/bbx108

Kumar S, Stecher G, Li M, Knyaz C, Tamura K. 2018. MEGA X: molecular evolutionary genetics analysis across computing platforms. Molecular Biology and Evolution 35, 1547. https://doi.org/10.1093%2Fmolbev%2Fmsy096

Lefort V, Longueville JE, Gascuel, O. 2017. SMS: smart model selection in PhyML. Molecular Biology and Evolution 34, 2422-2424. https://doi.org/10.1093/molbev/msx149

Lugtenberg BJ, Caradus JR, Johnson LJ. 2016. Fungal endophytes for sustainable crop production. FEMS Microbiology Ecology 92, fiw194. https://doi.org/10.1093/femsec/fiw194

MAFFT version 7. 2017. https://mafft.cbrc.jp/alignment/server/index.html (September 6, 2017).

Maldonado-Bonilla LD, Calderón-Oropeza MA, Villarruel-Ordaz JL, Sánchez-Espinosa AC. 2019. Identification of novel potential causal agents of *Fusarium* wilt of *Musa* sp. AAB in southern Mexico. Journal of Plant Pathology and Microbiology 10, e479. https://doi.org/10.35248/2157-7471.10.479

Maneeboon T, Sangchote S, Hongprayoon R, Chuaysrinule C, Mahakarnchanakul W. 2023. Occurrence of heat-resistant mold ascospores in pineapple and sugarcane field soils in Thailand. International Journal of Microbiology 23, 8347560. https://doi.org/10.1155/2023/8347560

ToupTek Photonics Co., Ltd. 2024. https://touptek-toupview.software.informer.com/3.7/ (November 4, 2023).

Matheny PB. 2005. Improving phylogenetic inference of mushrooms with *RPB1* and *RPB2* nucleotide sequences (*Inocybe*; Agaricales). Molecular Phylogenetics and Evolution 35, 1-20. https://doi.org/10.1016/j.ympev.2004.11.014

Naraghi L, Heydari A, Rezaee S, Razavi M. 2012. Biocontrol agent *Talaromyces flavus* stimulates the growth of cotton and potato. Journal of Plant Growth Regulation 31, 471-477. https://doi.org/10.1007/s00344-011-9256-2

Ortega-Acosta SA, Reyes-García G, Vargas-Álvarez D, Gámez-Vázquez AJ, Ávila-Perches MA, Espinosa-Trujillo E, Bello-Martínez J, Damián-Nava A, Palemón-Alberto F. 2018. First report of *Talaromyces verruculosus* causing storage rot of groundnut in Mexico. New Disease Reports 38, 27. http://dx.doi.org/10.5197/j.2044-0588.2018.038.027

Pitt JI. 1979. The genus *Penicillium* and its teleomorphic states *Eupenicillium* and *Talaromyces*. Academic Press Inc. Ltd., Cambridge.

Ronquist F, Teslenko M, Van Der Mark P, Ayres DL, Darling A, Höhna S, Larget B, Liu L, Suchard MA, Huelsenbeck JP. 2012. MrBayes 3.2: efficient Bayesian phylogenetic inference and model choice across a large model space. Systematic Biology 61, 539-542. https://doi.org/10.1093/sysbio/sys029

Sun BD, Chen AJ, Houbraken J, Frisvad JC, Wu WP, Wei HL, Zhou YG, Jiang XZ, Samson RA. 2020. New section and species in *Talaromyces*. MycoKeys 68, 75. https://doi.org/10.3897%2Fmycokeys.68.52092

Sun XR, Xu MY, Kong WL, Wu F, Zhang Y, Xie XL, Li DW, Wu XQ. 2022.Fine identification and classification of a novel beneficial *Talaromyces* fungal species from Masson pine rhizosphere soil. Journal of Fungi 8, 155. https://doi.org/10.3390/jof8020155

Vinale F, Nicoletti R, Lacatena F, Marra R, Sacco A, Lombardi N, d'Errico G, Digilio MC, Lorito M. Woo SL. 2017. Secondary metabolites from the endophytic fungus *Talaromyces pinophilus*. Natural Product Research 31, 1778-1785. https://doi.org/10.1080/14786419.2017.1290624

Wang XC, Zhuang WY. 2022. New species of *Talaromyces* (Trichocomaceae, Eurotiales) from Southwestern China. Journal of Fungi 8, 647. https://doi.org/10.3390/jof8070647

Wei S, Xu X, Wang L. 2021. Four new species of *Talaromyces* section *Talaromyces* discovered in China. Mycologia 113, 492-508. https://doi.org/10.1080/00275514.2020.1853457

Yilmaz N, Visagie CM, Houbraken J, Frisvad JC, Samson RA. 2014. Polyphasic taxonomy of the genus *Talaromyces*. Studies in Mycology 78, 175-341. https://doi.org/10.1016/j.simyco.2014.08.001